

# Prompt $J/\psi$ production at LHC: new evidence for the $k_T$ -factorization

S.P. Baranov<sup>a</sup>, A.V. Lipatov<sup>b</sup>, N.P. Zotov<sup>b</sup>

August 9, 2018

<sup>a</sup> *P.N. Lebedev Physics Institute,  
119991 Moscow, Russia*

<sup>b</sup> *D.V. Skobeltsyn Institute of Nuclear Physics,  
M.V. Lomonosov Moscow State University,  
119991 Moscow, Russia*

## Abstract

In the framework of the  $k_T$ -factorization approach, the production and polarization of prompt  $J/\psi$  mesons in  $pp$  collisions at the LHC energy  $\sqrt{s} = 7$  TeV is studied. Both the direct production mechanism as well as feed-down contributions from  $\chi_{c1}$ ,  $\chi_{c2}$  and  $\psi'$  decays are taken into account. Our consideration is based on the color singlet model supplemented with the off-shell matrix elements for the corresponding partonic subprocesses. The unintegrated gluon densities in a proton are determined using the CCFM evolution equation as well the Kimber-Martin-Ryskin prescription. We compare our numerical predictions with the first experimental data taken by the CMS, ATLAS and LHCb collaborations. The estimation of polarization parameters  $\lambda_\theta$ ,  $\lambda_\phi$  and  $\lambda_{\theta\phi}$  which determine  $J/\psi$  spin density matrix is performed.

PACS number(s): 12.38.-t, 13.20.Gd, 13.88.+e

## 1 Introduction

The production of charmonium states at high energies is under intense theoretical and experimental study [1–3]. The production mechanism involves the physics of both short and long distances, and so, appeals to both perturbative and nonperturbative methods of QCD.

This feature gives rise to two competing theoretical approaches known in the literature as the color singlet (CS) [4] and color octet (CO) [5] models. In the CS model, only those states with the same quantum numbers as the resulting charmonium contribute to the formation of a bound state. This is achieved by radiating a hard gluon in a perturbative process. In the CO model, it was suggested to add the contribution of transition mechanism from  $c\bar{c}$  pairs to charmonium, where a charmed quark pair is produced in a color octet state and transforms into the final color singlet state by the help of soft gluon radiation. The CO model is based on the general principle of the non-relativistic QCD factorization (NRQCD) [6]. As it is well known, the sole leading order (LO) CS model is insufficient to describe the experimental data on the  $J/\psi$  production at the Tevatron energies. By adding the contribution from the octet states and fitting the free parameters one was able to describe the data on the  $J/\psi$  production at energies of modern colliders (see [7] and references therein).

However, recently the next-to-leading order (NLO) [8] and dominant next-to-next-to-leading order (NNLO\*) [9] corrections to the CS mechanism have been calculated and have been found to be essential in description of quarkonia production. The comparison with the first LHC measurements performed by the ATLAS, CMS and LHCb collaborations demonstrates [10] that the NNLO\* CS model correctly reproduces the transverse momentum distributions as well as the total cross section of  $J/\psi$  mesons at  $\sqrt{s} = 7$  TeV.

The effect of high-order QCD corrections is also manifest in the polarisation predictions. While the charmonium produced inclusively or in association with a photon are predicted to be transversely polarised at LO, it has been found that their polarisation at NLO is increasingly longitudinal at high  $p_T$  [9, 11]. Opposite, the NRQCD predicts the strong transverse polarization of the final state quarkonia [1]. This is in disagreement with the polarisation measurement [12] performed by the CDF collaboration at the Tevatron, casting doubt on the earlier conclusion that the CO terms dominate  $J/\psi$  production.

The results of studies [8–11] support the predictions [13–22] obtained in the framework of the  $k_T$ -factorization QCD approach [23], where investigations of heavy quarkonia production and polarization have own long story. Shortly, it was demonstrated [14–21] that the experimental data on quarkonia production at HERA, RHIC and Tevatron can be well described within the CS model alone. The values of CO contributions obtained by fitting the Tevatron data appear to be substantially smaller than the ones in the NRQCD formalism [14, 16, 24]. Furthermore, the longitudinal polarization of produced  $J/\psi$  mesons predicted by the  $k_T$ -factorization is an immediate consequence of initial gluon off-shellness [14] which taken into account in the  $k_T$ -factorization approach<sup>1</sup>.

In the present note we give the systematic analysis<sup>2</sup> of first experimental data [26–28] on the prompt  $J/\psi$  production taken by the CMS, ATLAS and LHCb collaborations at the LHC energy  $\sqrt{s} = 7$  TeV. Follow the guideline of previous studies [19, 20], in our consideration we will apply the CS model supplemented with the  $k_T$ -factorization approach. Two sources of  $J/\psi$  production are taken into account: direct  $J/\psi$  production and feed-down  $J/\psi$  from the decay of other heavier prompt charmonium states like  $\chi_{c1}$ ,  $\chi_{c2}$  or  $\psi'$ , that is in a full agreement with the experimental setup [26–28]. Specially we concentrate on the  $J/\psi$  spin alignment and estimate three polarization parameters  $\lambda_\theta$ ,  $\lambda_\phi$  and  $\lambda_{\theta\phi}$  defining the spin density matrix

---

<sup>1</sup>A detailed description and discussion of the  $k_T$ -factorization approach can be found, for example, in reviews [27].

<sup>2</sup>See also [22].

of produced  $J/\psi$  mesons. As it was mentioned above, studies of polarization observables are useful in discriminating the CS and CO production mechanisms,

The outline of our paper is following. In Section 2 we recall shortly the basic formulas of the  $k_T$ -factorization approach with a brief review of calculation steps. In Section 3 we present the numerical results of our calculations and a discussion. Section 4 contains our conclusions.

## 2 Theoretical framework

The production of prompt  $J/\psi$  mesons in  $pp$  collisions at the LHC can proceed via either direct gluon-gluon fusion or the production of heavier  $P$ -wave states  $\chi_{cJ}$  ( $J = 0, 1, 2$ ) and  $S$ -wave state  $\psi'$ , followed by their radiative decays  $\chi_{cJ} \rightarrow J/\psi + \gamma$  and  $\psi' \rightarrow J/\psi + X$ . In the CS model, the direct mechanism corresponds to the partonic subprocess  $g^* + g^* \rightarrow J/\psi + g$  which includes the emission of an additional hard gluon in the final state. The production of  $P$ -wave quarkonia is given by  $g^* + g^* \rightarrow \chi_{cJ}$  [21] and there is no emission of any additional gluons. The feed-down contribution from  $S$ -wave state  $\psi'$  is described by the  $g^* + g^* \rightarrow \psi' + g$  subprocess.

The production amplitudes of all these subprocesses can be obtained from the one for an unspecified  $c\bar{c}$  state by the application of appropriate projection operators  $J(S, L)$  which guarantee the proper quantum numbers of the  $c\bar{c}$  state under consideration. These operators for the different spin and orbital angular momentum states can be written as [4]

$$J(^3S_1) = J(S = 1, L = 0) = \hat{\epsilon}(S_z)(\hat{p}_c + m_c)/m^{1/2}, \quad (1)$$

$$J(^3P_J) = J(S = 1, L = 1) = (\hat{p}_{\bar{c}} - m_c)\hat{\epsilon}(S_z)(\hat{p}_c + m_c)/m^{3/2}, \quad (2)$$

where  $m$  is the mass of the specifically considered  $c\bar{c}$  state,  $p_c$  and  $p_{\bar{c}}$  are the four-momenta of the charmed quark and anti-quark. In accordance with the non-relativistic formalism of bound state formation, the charmed quark mass  $m_c$  is always set equal to 1/2 of the quarkonium mass. States with various projections of the spin momentum onto the  $z$  axis are represented by the polarization vector  $\epsilon(S_z)$ .

The probability for the two quarks to form a meson depends on the bound state wave function  $\Psi(q)$ . In the non-relativistic approximation, the relative momentum  $q$  of the quarks in the bound state is treated as a small quantity. So, we represent the quark momenta as follows:

$$p_c = p/2 + q, \quad p_{\bar{c}} = p/2 - q, \quad (3)$$

where  $p$  is the four-momentum of the final state quarkonium. Then, we multiply the relevant partonic amplitude  $\mathcal{A}$  (depending on  $q$ ) by  $\Psi(q)$  and perform integration with respect to  $q$ . The integration is performed after expanding the integrand around  $q = 0$ :

$$\mathcal{A}(q) = \mathcal{A}|_{q=0} + q^\alpha(\partial\mathcal{A}/\partial q^\alpha)|_{q=0} + \dots, \quad (4)$$

Since the expressions for  $\mathcal{A}|_{q=0}$  and  $\partial\mathcal{A}/\partial q^\alpha|_{q=0}$  are no longer dependent on  $q$ , they may be factored outside the integral sign. A term-by-term integration of this series then yields [29]

$$\int \frac{d^3q}{(2\pi)^3} \Psi(q) = \frac{1}{\sqrt{4\pi}} \mathcal{R}(x = 0), \quad (5)$$

$$\int \frac{d^3q}{(2\pi)^3} q^\alpha \Psi(q) = -i\epsilon^\alpha(L_z) \frac{\sqrt{3}}{\sqrt{4\pi}} \mathcal{R}'(x=0), \quad (6)$$

where  $\mathcal{R}(x)$  is the radial wave function in the coordinate representation, i.e. the Fourier transform of  $\Psi(q)$ . The first term in (4) contributes only to  $S$  waves, but vanishes for  $P$  waves because  $\mathcal{R}_P(0) = 0$ . On the contrary, the second term contributes only to  $P$  waves, but vanishes for  $S$  waves because  $\mathcal{R}'_S(0) = 0$ . States with various projections of the orbital angular momentum onto the  $z$  axis are represented by the polarization vector  $\epsilon(L_z)$ . The numerical values of the wave functions are either known from the leptonic decay widths (for  $J/\psi$  and  $\psi'$  mesons) or can be taken from potential models (for  $\chi_{cJ}$  mesons).

In our numerical calculations, the polarization vectors  $\epsilon(S_z)$  and  $\epsilon(L_z)$  are defined as explicit four-vectors. In the frame where the  $z$  axis is oriented along the quarkonium momentum vector  $p^\mu = (E, 0, 0, |\mathbf{p}|)$ , these polarization vectors read

$$\epsilon^\mu(\pm 1) = (0, \pm 1, i, 0)/\sqrt{2}, \quad \epsilon^\mu(0) = (|\mathbf{p}|, 0, 0, E)/m. \quad (7)$$

The states with definite  $S_z$  and  $L_z$  are translated into states with definite total momentum  $J$  and its projection  $J_z$  using the Clebsch-Gordan coefficients:

$$\epsilon^{\mu\nu}(J, J_z) = \sum_{S_z, L_z} \langle 1, L_z; 1, S_z | J, J_z \rangle \epsilon^\mu(S_z) \epsilon^\nu(L_z). \quad (8)$$

Further evaluation of all partonic amplitudes under consideration (including subsequent leptonic and/or radiative decays, of course) is straightforward and was done using the algebraic manipulation systems FORM [30]. We do not list here the obvious expressions because lack of space, but only mention several technical points. First, in according to the  $k_T$ -factorization prescription [23], the summation over the incoming off-shell gluon polarizations is carried with  $\sum \epsilon^\mu \epsilon^{*\nu} = \mathbf{k}_T^\mu \mathbf{k}_T^\nu / \mathbf{k}_T^2$ , where  $\mathbf{k}_T$  is the gluon transverse momentum orthogonal to the beam axis. In the collinear limit, when  $|\mathbf{k}_T| \rightarrow 0$ , this expression converges to the ordinary  $\sum \epsilon^\mu \epsilon^{*\nu} = -g^{\mu\nu}/2$  after averaging on the azimuthal angle. In all other respects the evaluation follows the standard QCD Feynman rules. Second, the spin density matrix of final  $J/\psi$  meson is determined by the momenta  $l_1$  and  $l_2$  of the decay leptons and is taken in the form

$$\sum \epsilon^\mu \epsilon^{*\nu} = 3 \left( l_1^\mu l_2^\nu + l_1^\nu l_2^\mu - \frac{m^2}{2} g^{\mu\nu} \right) / m^2. \quad (9)$$

This expression is equivalent to the standard one  $\sum \epsilon^\mu \epsilon^{*\nu} = -g^{\mu\nu} + p^\mu p^\nu / m^2$  but is better suited for studying the polarization observables because it gives access to the kinematic variables describing the orientation of the decay plane. Third, when considering the polarization properties of  $J/\psi$  mesons originating from radiative decays of  $P$ -wave states, we rely upon the dominance of electric dipole  $E1$  transitions<sup>3</sup>. The corresponding invariant amplitudes can be written as [31]

$$i\mathcal{A}(\chi_{c1} \rightarrow J/\psi + \gamma) = g_1 \epsilon^{\mu\nu\alpha\beta} k_\mu \epsilon_\nu^{(\chi_{c1})} \epsilon_\alpha^{(J/\psi)} \epsilon_\beta^{(\gamma)}, \quad (10)$$

$$i\mathcal{A}(\chi_{c2} \rightarrow J/\psi + \gamma) = g_2 p^\mu \epsilon_{(\chi_{c2})}^{\alpha\beta} \epsilon_\alpha^{(J/\psi)} \left[ k_\mu \epsilon_\beta^{(\gamma)} - k_\beta \epsilon_\mu^{(\gamma)} \right], \quad (11)$$

---

<sup>3</sup>The same approach has been applied [19] to study the  $\Upsilon$  production and polarization at the Tevatron.

where  $\epsilon_\mu^{(\chi_{c1})}$ ,  $\epsilon_\mu^{(J/\psi)}$  and  $\epsilon_\mu^{(\gamma)}$  are the polarization vectors of a corresponding spin-one particles and  $\epsilon_{\mu\nu}^{(\chi_{c2})}$  is its counterpart for a spin-two  $\chi_{c2}$  meson,  $p$  and  $k$  are the four-momenta of the decaying quarkonium and the emitted photon,  $\epsilon^{\mu\nu\alpha\beta}$  is the fully antisymmetric Levita-Civita tensor. The dominance of electric dipole transitions for the charmonium family is supported by the experimental data taken by the E835 Collaboration at the Tevatron [32]. Since the electromagnetic branching ratio for  $\chi_{c0} \rightarrow J/\psi + \gamma$  decay is more than an order of magnitude smaller than those for  $\chi_{c1}$  and  $\chi_{c2}$ , we neglect its contribution to  $J/\psi$  production. As the  $\psi' \rightarrow J/\psi + X$  decay matrix elements are unknown, these events were generated according to the phase space.

The cross section of  $J/\psi$  production at high energies in the  $k_T$ -factorization approach is calculated as a convolution of the off-shell partonic cross section and the unintegrated gluon distributions in a proton. The contribution from the direct production mechanism can be presented in the following form:

$$\begin{aligned} \sigma(pp \rightarrow J/\psi + X) &= \int \frac{1}{16\pi(x_1x_2s)^2} f_g(x_1, \mathbf{k}_{1T}^2, \mu^2) f_g(x_2, \mathbf{k}_{2T}^2, \mu^2) \times \\ &\times |\bar{\mathcal{M}}(g^* + g^* \rightarrow J/\psi + g)|^2 d\mathbf{p}_T^2 d\mathbf{k}_{1T}^2 d\mathbf{k}_{2T}^2 dy dy_g \frac{d\phi_1}{2\pi} \frac{d\phi_2}{2\pi}, \end{aligned} \quad (12)$$

where  $f_g(x, \mathbf{k}_T^2, \mu^2)$  is the unintegrated gluon density,  $\mathbf{p}_T$  and  $y$  are the transverse momentum and rapidity of produced  $J/\psi$  meson,  $y_g$  is the rapidity of outgoing gluon and  $s$  is the  $pp$  center-of-mass energy. The initial off-shell gluons have a fraction  $x_1$  and  $x_2$  of the parent protons longitudinal momenta, non-zero transverse momenta  $\mathbf{k}_{1T}$  and  $\mathbf{k}_{2T}$  ( $\mathbf{k}_{1T}^2 = -k_{1T}^2 \neq 0$ ,  $\mathbf{k}_{2T}^2 = -k_{2T}^2 \neq 0$ ) and azimuthal angles  $\phi_1$  and  $\phi_2$ . For the production of  $\chi_{cJ}$  mesons via  $2 \rightarrow 1$  subprocess above we have

$$\begin{aligned} \sigma(pp \rightarrow \chi_{cJ} + X) &= \int \frac{2\pi}{x_1x_2sT} f_g(x_1, \mathbf{k}_{1T}^2, \mu^2) f_g(x_2, \mathbf{k}_{2T}^2, \mu^2) \times \\ &\times |\bar{\mathcal{M}}(g^* + g^* \rightarrow \chi_{cJ})|^2 d\mathbf{k}_{1T}^2 d\mathbf{k}_{2T}^2 dy \frac{d\phi_1}{2\pi} \frac{d\phi_2}{2\pi}, \end{aligned} \quad (13)$$

where  $T$  is the off-shell gluon flux factor. In the present analysis we set it to be equal to  $T = 2\hat{s}$ , where  $\hat{s}$  is the energy of partonic subprocess. In (12) and (13),  $|\bar{\mathcal{M}}(g^* + g^* \rightarrow J/\psi + g)|^2$  and  $|\bar{\mathcal{M}}(g^* + g^* \rightarrow \chi_{cJ})|^2$  are the corresponding off-shell matrix elements squared and averaged over initial gluon polarizations and colors. The production scheme of  $\psi'$  meson is identical to that of  $J/\psi$ , and only the numerical value of the wave function  $|\mathcal{R}(0)|^2$  is different (see below).

In the numerical calculations we have tested a few different sets of unintegrated gluon distributions involved in (12) and (13). First of them (CCFM set A0) has been obtained [33] from the CCFM equation where all input parameters have been fitted to describe the proton structure function  $F_2(x, Q^2)$ . Equally good fit of the  $F_2$  data was obtained using different values for the soft cut and a different value for the width of the intrinsic  $\mathbf{k}_T$  distribution (CCFM set B0). Also we will use the unintegrated gluons taken in the Kimber-Martin-Ryskin (KMR) form [34]. The KMR approach is a formalism to construct the unintegrated parton distributions from well-known conventional ones. For the input, we have used recent leading-order Martin-Stirling-Thorn-Watt (MSTW) set [35].

The multidimensional integrations in (12) and (13) have been performed by the means of Monte Carlo technique, using the routine VEGAS [36]. The full C++ code is available from the author on request<sup>4</sup>.

### 3 Numerical results

We now are in a position to present our numerical results. First we describe our input and the kinematic conditions. After we fixed the unintegrated gluon distributions, the cross sections (12) and (13) depend on the renormalization and factorization scales  $\mu_R$  and  $\mu_F$ . Numerically, we set  $\mu_R^2 = m^2 + \mathbf{p}_T^2$  and  $\mu_F^2 = \hat{s} + \mathbf{Q}_T^2$ , where  $\mathbf{Q}_T$  is the transverse momentum of initial off-shell gluon pair. Note that the choice of  $\mu_R$  is the standard one for studying of the  $J/\psi$  production whereas the special choice of  $\mu_F$  is connected with the CCFM evolution (see [33]). Following to [37], we set  $m_{J/\psi} = 3.097$  GeV,  $m_{\chi_{c1}} = 3.511$  GeV,  $m_{\chi_{c2}} = 3.556$  GeV,  $m_{\psi'} = 3.686$  GeV and use the LO formula for the coupling constant  $\alpha_s(\mu^2)$  with  $n_f = 4$  quark flavours at  $\Lambda_{\text{QCD}} = 200$  MeV, such that  $\alpha_s(M_Z^2) = 0.1232$ . The charmonia wave functions at the origin of coordinate space are taken to be equal to  $|\mathcal{R}_{J/\psi}(0)|^2 = 0.0876$  GeV<sup>3</sup> [37],  $|\mathcal{R}'_{\chi}(0)|^2 = 0.075$  GeV<sup>5</sup> [38],  $|\mathcal{R}_{\psi'}(0)|^2 = 0.0391$  GeV<sup>3</sup> [37]. According to [37], the following branching fractions are used:  $B(\chi_{c1} \rightarrow J/\psi + \gamma) = 0.356$ ,  $B(\chi_{c2} \rightarrow J/\psi + \gamma) = 0.202$ ,  $B(\psi' \rightarrow J/\psi + X) = 0.561$  and  $B(J/\psi \rightarrow \mu^+ \mu^-) = 0.0593$ .

The results of our calculations are presented in Figs. 1 — 3 in comparison with the CMS, ATLAS and LHCb data [26–28]. The solid, dashed and dash-dotted curves correspond to the results obtained using the CCFM A0, B0 and KMR gluon densities, respectively. Everywhere, we separately show the contribution from the direct production mechanism taken solely (dotted curves). In this case we apply the CCFM A0 gluon density for illustration. It is clear that sole direct production is not sufficient to describe the LHC data. However, we obtain a good overall agreement of our predictions and the data when summing up the direct and feed-down contributions. The latter is important and production of  $J/\psi$  mesons via radiative decays of  $\chi_{cJ}$  and  $\psi'$  mesons even dominates over the direct contribution at large transverse momenta. The reason can be seen in the fact that the production of  $\chi_{cJ}$  states refers to much lower values of the final state invariant mass and therefore effectively probes small  $x$  region, where the gluon distributions are growing up. The dependence of our numerical results on the unintegrated PDFs is rather weak and the CCFM and KMR predictions are practically coincide. The difference between them can be observed at small  $p_T$  or at large rapidities probed at the LHCb measurements.

Computations [7] performed in the framework of NRQCD, where CO contributions are taken into account, can also explain at satisfactory level the shape and the absolute normalization of the measured  $J/\psi$  cross-sections. However, as it was mentioned above, they predict a substantial transverse component for the polarisation of  $J/\psi$  mesons at large  $p_T$  which is not supported by measurements. We find that in the framework of the  $k_T$ -factorization approach no need for a CO contributions in the description of  $J/\psi$  production at the LHC. From the other side, the account of high-order corrections to the CS cross sections calculated in the collinear QCD factorization also leads to the significant improvements in description of the data: the upper bound of the NNLO\* CS predictions is very close [11] to the mea-

---

<sup>4</sup>lipatov@theory.sinp.msu.ru

Source	$\lambda_\theta$ (HX)	$\lambda_\phi$ (HX)	$\lambda_{\theta\phi}$ (HX)	$\lambda_\theta$ (CS)	$\lambda_\phi$ (CS)	$\lambda_{\theta\phi}$ (CS)
Direct	-0.15	-0.09	0.01	0.20	-0.22	-0.01
Feed-down	0.19	0.14	0.00	0.35	0.09	0.00
Total	-0.07	-0.03	0.01	0.24	-0.14	-0.01

Table 1: The polarization parameters of prompt  $J/\psi$  mesons calculated in the kinematical region of CMS and ATLAS measurements [26, 27]. The CCFM A0 gluon density is used.

measurements [26–28] and agree much better (compared to the LO CS results) with the  $k_T$ -factorization calculations which incorporates a large part of collinear high-order corrections at LO level.

Note that the calculated cross sections of feed-down contributions from the  $P$ -wave states are free from singularities at small transverse momenta. This contrasts with the collinear QCD factorization predictions, which are either unphysical or even divergent.

Now we turn to the  $J/\psi$  polarization. In general, the spin density matrix of a vector particle depends on three parameters  $\lambda_\theta$ ,  $\lambda_\phi$  and  $\lambda_{\theta\phi}$  which can be measured experimentally. So, the double differential angular distribution of the  $J/\psi \rightarrow \mu^+\mu^-$  decay products reads [39]

$$\frac{d\sigma}{d\cos\theta^*d\phi^*} \sim 1 + \lambda_\theta \cos^2\theta^* + \lambda_\phi \sin^2\theta^* \cos 2\phi^* + \lambda_{\theta\phi} \sin 2\theta^* \cos \phi^*, \quad (14)$$

where  $\theta^*$  and  $\phi^*$  are the polar and azimuthal angles of the decay lepton measured in the  $J/\psi$  rest frame. Since the polarization parameters  $\lambda_\theta$ ,  $\lambda_\phi$  and  $\lambda_{\theta\phi}$  (which greatly affects on the cross sections) are not determined yet at the LHC, the results of measurements performed by the CMS, ATLAS and LHCb collaborations have been presented in a different ways. So, in the ATLAS analysis [27] the unknown  $J/\psi$  polarization has been treated as an additional source of systematic uncertainties. Contrary, the CMS and LHCb collaborations quote their measurements [26, 28] for different polarization scenarios: unpolarized ( $\lambda_\theta = 0$ ), full longitudinal polarization ( $\lambda_\theta = -1$ ) and full transverse  $J/\psi$  polarization ( $\lambda_\theta = 1$ ) in the Collins-Soper or the helicity frames<sup>5</sup>. Below we estimate the polarization parameters  $\lambda_\theta$ ,  $\lambda_\phi$  and  $\lambda_{\theta\phi}$  in a whole kinematical regions regarding the CMS, ATLAS and LHCb measurements. Our evaluation is generally followed the experimental procedure. We have collected the simulated events in the specified bins of  $J/\psi$  transverse momentum  $p_T$  and rapidity  $y$ , generated the decay lepton angular distributions according to the production and decay matrix elements, and then applied a three-parametric fit based on (14). The estimated values of polarization parameters  $\lambda_\theta$ ,  $\lambda_\phi$  and  $\lambda_{\theta\phi}$  in the helicity (HX) and Collins-Soper (CS) frames

<sup>5</sup>The experimental data points in Figs. 1 and 3 correspond to the unpolarized scenario.

Source	$\lambda_\theta$ (HX)	$\lambda_\phi$ (HX)	$\lambda_{\theta\phi}$ (HX)	$\lambda_\theta$ (CS)	$\lambda_\phi$ (CS)	$\lambda_{\theta\phi}$ (CS)
Direct	-0.03	-0.13	0.17	0.19	-0.22	-0.03
Feed-down	0.22	0.11	0.13	0.43	0.05	0.05
Total	0.03	-0.07	0.16	0.26	-0.14	-0.01

Table 2: The polarization parameters of prompt  $J/\psi$  mesons calculated in the kinematical region of LHCb measurements [28]. The CCFM A0 gluon density is used.

are listed in Tables 1 and 2. We find that these parameters are the same in the kinematical regions covered by the CMS and ATLAS collaborations. In order to study the production dynamics in more detail, we separately show contributions from the direct and feed-down mechanisms. The latter, of course, change the polarization of final  $J/\psi$  mesons predicted by the direct production mechanism [19] but this effect is not well pronounced due to overall integration over  $J/\psi$  transverse momentum. Note that the qualitative predictions for the  $J/\psi$  polarization are stable with respect to variations in the model parameters. In fact, there is no dependence on the strong coupling constant and unintegrated gluon densities, i.e. two of an important sources of theoretical uncertainties cancels out. Therefore future precise measurements of the polarization parameters at the LHC will play crucial role in discriminating the different theoretical approaches.

## 4 Conclusions

We have investigated prompt  $J/\psi$  production in  $pp$  collisions at the LHC energy  $\sqrt{s} = 7$  TeV within the framework of the  $k_T$ -factorization approach. Both the direct production mechanism as well as feed-down contributions from  $\chi_{c1}$ ,  $\chi_{c2}$  and  $\psi'$  decays are taken into account. Our consideration is based on the color singlet model supplemented with the off-shell matrix elements for the corresponding partonic subprocesses. The unintegrated gluon densities in a proton are determined using the CCFM evolution equation as well the Kimber-Martin-Ryskin prescription. We have obtained well agreement of our calculations and the first experimental data taken by the CMS and ATLAS collaborations when summing up the direct and feed-down contributions. The dependence of our predictions on the unintegrated gluon densities appears at small transverse momenta and at large rapidities covered by the LHCb experiment. We have demonstrated also that in the framework of the  $k_T$ -factorization there is no room for a color octet contributions for charmonium production at the LHC.

The estimation of the polarization parameters  $\lambda_\theta$ ,  $\lambda_\phi$  and  $\lambda_{\theta\phi}$  which determine the  $J/\psi$  spin density matrix is given. The future experimental analysis of the quarkonium polarization



at the LHC turned out to be very important and informative for discriminating the different theoretical models.

## 5 Acknowledgements

We are very grateful to DESY Directorate for the support in the framework of Moscow — DESY project on Monte-Carlo implementation for HERA — LHC. A.V.L. was supported in part by the grant of the President of Russian Federation (MK-3977.2011.2). Also this research was supported by the FASI of Russian Federation (grant NS-4142.2010.2), FASI state contract 02.740.11.0244 and RFBR grant 11-02-01454-a.

## References

- [1] M. Krämer, Prog. Part. Nucl. Phys. **47**, 141 (2001).
- [2] J.P. Lansberg, Int. J. Mod. Phys. A **21**, 3857 (2006).
- [3] N. Brambilla *et al.*, Eur. Phys. J. C **71**, 1534 (2011).
- [4] C.-H. Chang, Nucl. Phys. B **172**, 425 (1980);  
E.L. Berger and D.L. Jones, Phys. Rev. D **23**, 1521 (1981);  
R. Baier and R. Rückl, Phys. Lett. B **102**, 364 (1981);  
S.S. Gershtein, A.K. Likhoded, and S.R. Slabospitsky, Sov. J. Nucl. Phys. **34**, 128 (1981).
- [5] E. Braaten and S. Fleming, Phys. Rev. Lett. **74**, 3327 (1995).
- [6] G. Bodwin, E. Braaten, and G. Lepage, Phys. Rev. D **51**, 1125 (1995); Phys. Rev. D **55**, 5853 (1997).
- [7] M. Butenschoen and B.A. Kniehl, DESY 11-046; arXiv:1105.0820.
- [8] J. Campbell, F. Maltoni, and F. Tramontano, Phys. Rev. Lett. **98**, 252002 (2007).
- [9] P. Artoisenet, J. Campbell, J.P. Lansberg, F. Maltoni, and F. Tramontano, Phys. Rev. Lett. **101**, 152001 (2008).
- [10] J.P. Lansberg, in Proceedings of Quark Matter 2011; arXiv:1107.0292.
- [11] B. Gong and J.X. Wang, Phys. Rev. Lett. **100**, 232001 (2008); Phys. Rev. D **78**, 074011 (2008).
- [12] A. Abulencia *et al.* (CDF Collaboration), Phys. Rev. Lett. **99**, 132001 (2007).
- [13] S.P. Baranov, Phys. Lett. B **428**, 377 (1998).
- [14] S.P. Baranov, Phys. Rev. D **66**, 114003 (2002).

- [15] A.V. Lipatov and N.P. Zotov, Eur. Phys. J. C **27**, 87 (2003).
- [16] S.P. Baranov and N.P. Zotov, J. Phys. G **29**, 1395 (2003).
- [17] N.P. Zotov, I.I. Katkov, and A.V. Lipatov, Phys. Atom. Nucl. **69**, 2045 (2006).
- [18] S.P. Baranov and A. Szczurek, Phys. Rev. D **77**, 054016 (2008).
- [19] S.P. Baranov and N.P. Zotov, JETP Lett. **88**, 711 (2008).
- [20] S.P. Baranov, A.V. Lipatov, and N.P. Zotov, Eur. Phys. J. C **71**, 1631 (2011).
- [21] S.P. Baranov, Phys. Rev. D **83**, 034035 (2011).
- [22] H. Jung, M. Kraemer, A.V. Lipatov, and N.P. Zotov, arXiv:1107.4328 [hep-ph].
- [23] L.V. Gribov, E.M. Levin, and M.G. Ryskin, Phys. Rep. **100**, 1 (1983);  
E.M. Levin, M.G. Ryskin, Yu.M. Shabelsky and A.G. Shuvaev, Sov. J. Nucl. Phys. **53**,  
657 (1991);  
S. Catani, M. Ciafaloni and F. Hautmann, Nucl. Phys. B **366**, 135 (1991);  
J.C. Collins and R.K. Ellis, Nucl. Phys. B **360**, 3 (1991).
- [24] B.A. Kniehl, D.V. Vasin, and V.A. Saleev, Phys. Rev. D **73**, 074022 (2006).
- [25] B. Andersson *et al.* (Small- $x$  Collaboration), Eur. Phys. J. C **25**, 77 (2002);  
J. Andersen *et al.* (Small- $x$  Collaboration), Eur. Phys. J. C **35**, 67 (2004);  
J. Andersen *et al.* (Small- $x$  Collaboration), Eur. Phys. J. C **48**, 53 (2006).
- [26] CMS Collaboration; arXiv:1011.4193.
- [27] G. Aad *et al.* (ATLAS Collaboration); arXiv:1104.3038.
- [28] R. Aaij *et al.* (LHCb Collaboration); arXiv:1103.0423.
- [29] H. Krasemann, Z. Phys. C **1**, 189 (1979);  
G. Guberina, J. Kuhn, R. Peccei, and R. Ruckl, Nucl. Phys. B **174**, 317 (1980).
- [30] J.A.M. Vermaseren, NIKHEF-00-023 .
- [31] P. Cho, M. Wise, and S. Trivedi, Phys. Rev. D **51**, R2039 (1995).
- [32] M. Ambrogiani *et al.* (E835 Collaboration), Phys. Rev. D **65**, 052002 (2002).
- [33] H. Jung, arXiv:hep-ph/0411287.
- [34] M.A. Kimber, A.D. Martin and M.G. Ryskin, Phys. Rev. D **63**, 114027 (2001);  
G. Watt, A.D. Martin and M.G. Ryskin, Eur. Phys. J. C **31**, 73 (2003).
- [35] A.D. Martin, W.J. Stirling, R.S. Thorne, and G. Watt, Eur. Phys. J. C **63**, 189 (2009).
- [36] G.P. Lepage, J. Comput. Phys. **27**, 192 (1978).

- [37] C. Amsler *et al.* (PDG Collaboration), Phys. Lett. B **667**, 1 (2008).
- [38] E.J. Eichten and C. Quigg, Phys. Rev. D **52**, 1726 (1995).
- [39] M. Beneke, M. Krämer, and M. Vanttinen, Phys. Rev. D **57**, 4258 (1998).

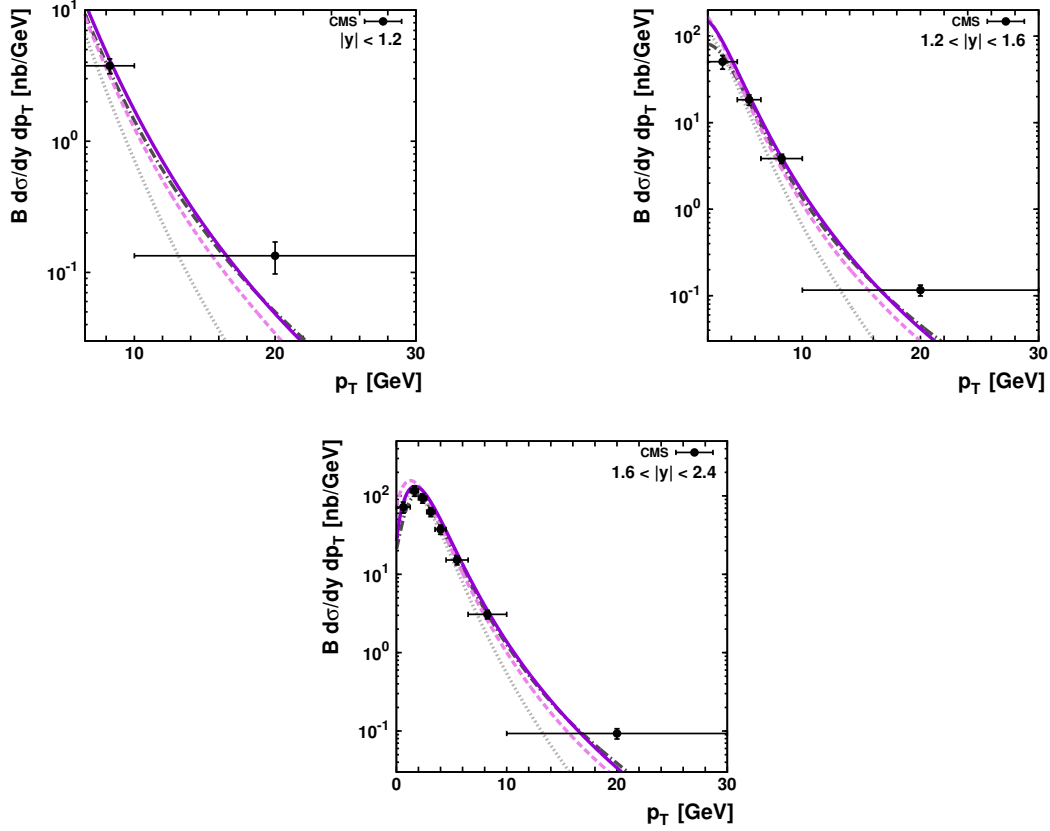


Figure 1: The double differential cross sections  $d\sigma/dydp_T$  of prompt  $J/\psi$  production at  $\sqrt{s} = 7$  TeV compared to the CMS data [26]. The solid, dashed and dash-dotted curves correspond to the results obtained using the CCFM A0, CCFM B0 and KMR gluon densities, respectively. The dotted curves represent the contribution from sole direct production mechanism calculated with the CCFM A0 gluon distribution.

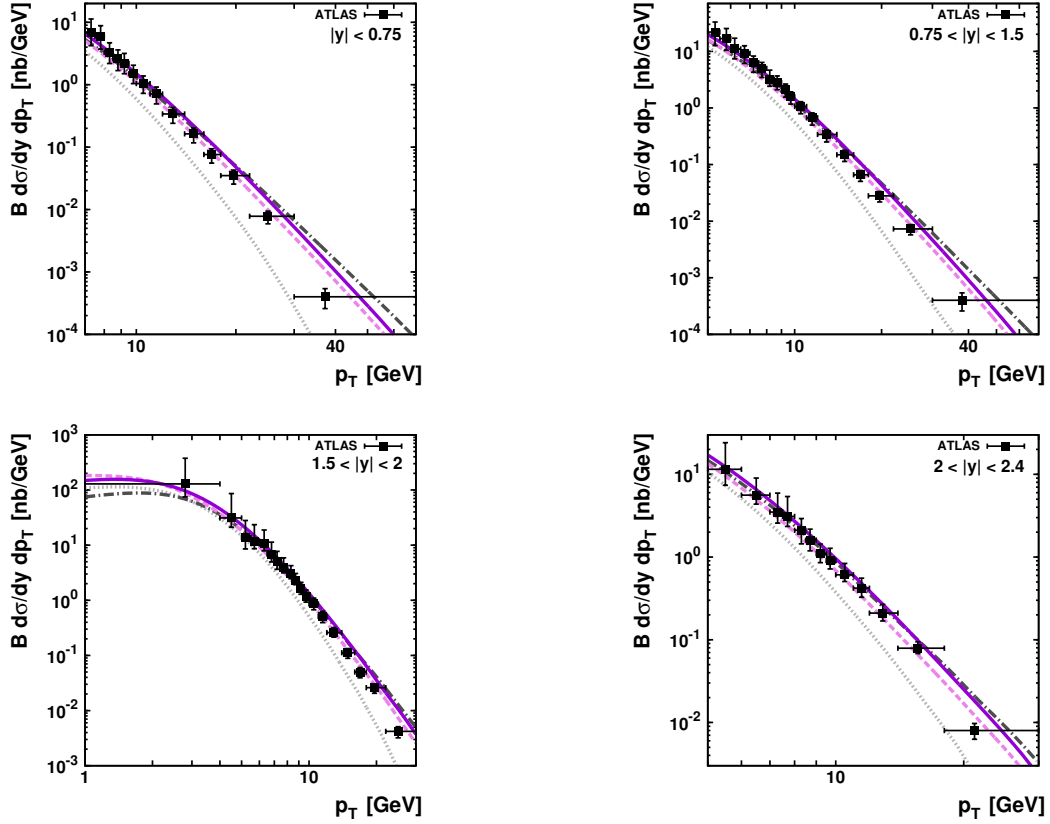


Figure 2: The double differential cross sections  $d\sigma/dydp_T$  of prompt  $J/\psi$  production at  $\sqrt{s} = 7$  TeV compared to the ATLAS data [27]. Notation of all histograms is the same as in Fig. 1.

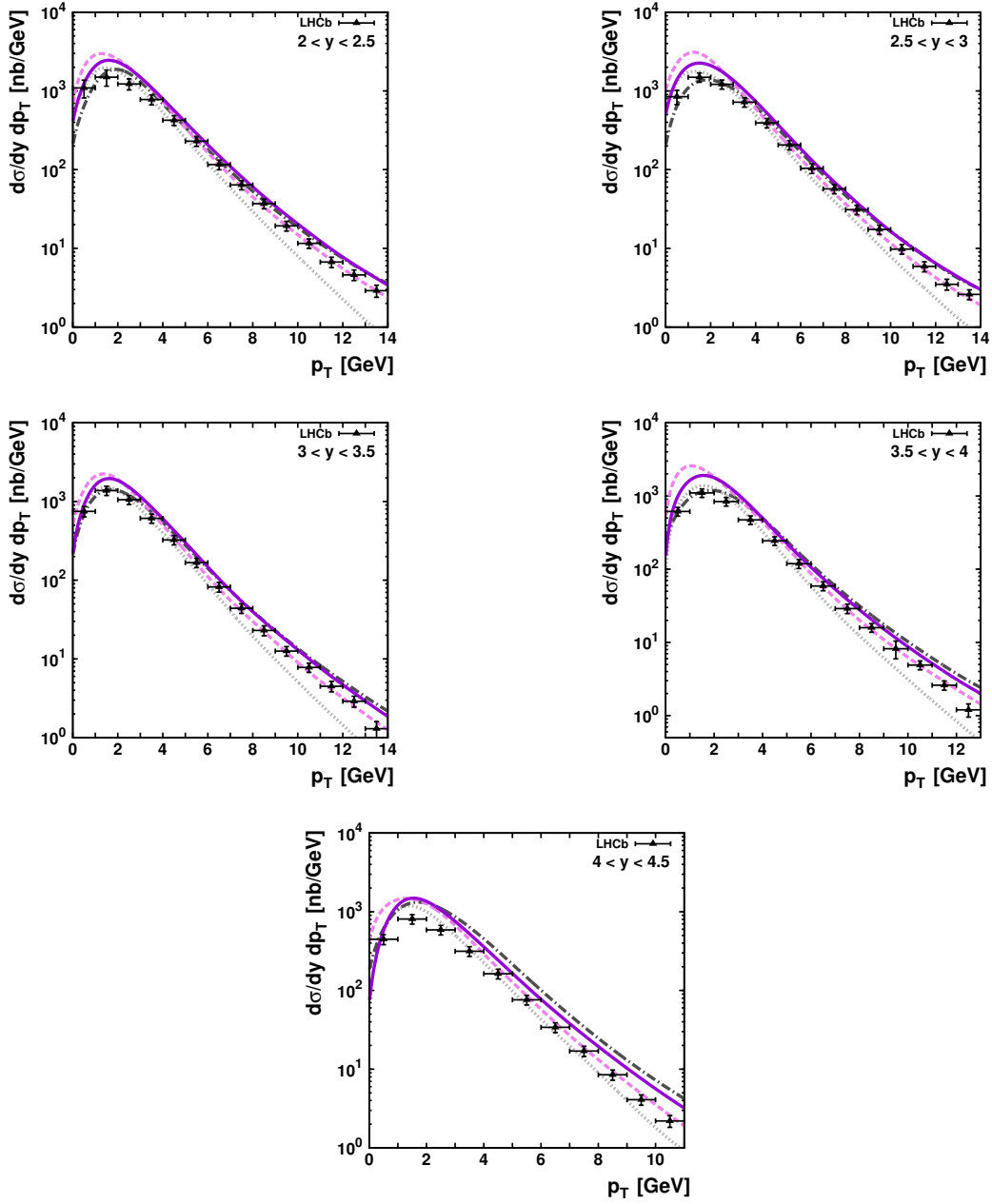


Figure 3: The double differential cross sections  $d\sigma/dy dp_T$  of prompt  $J/\psi$  production at  $\sqrt{s} = 7$  TeV compared to the LHCb data [28]. Notation of all histograms is the same as in Fig. 1.